

9-15-1998

Chemical signals from submarine fluid advection onto the continental shelf

W. S. Moore

University of South Carolina - Columbia, moore@geol.sc.edu

Timothy J. Shaw

University of South Carolina - Columbia, shaw@chem.sc.edu

Follow this and additional works at: https://scholarcommons.sc.edu/chem_facpub

 Part of the [Biological and Chemical Physics Commons](#), [Geophysics and Seismology Commons](#), [Oceanography Commons](#), and the [Physical Chemistry Commons](#)

Publication Info

Published in *Journal of Geophysical Research: Oceans*, Volume 103, Issue C10, 1998, pages 21543-21552.

An edited version of this paper was published by AGU. Copyright 1998 American Geophysical Union

Moore, W. S. & Shaw, T. J. (15 September 1998). Chemical signals from submarine fluid advection onto the continental shelf. *Journal of Geophysical Research: Oceans*, 103(C10), 21543-21552.

<http://dx.doi.org/10.1029/98JC02232>

Chemical signals from submarine fluid advection onto the continental shelf

Willard S. Moore

Department of Geological Sciences, University of South Carolina, Columbia

Timothy J. Shaw

Department of Chemistry and Biochemistry, University of South Carolina, Columbia

Abstract. We report unambiguous signals of subsurface fluid input on the continental shelf 40–80 km from shore in water depths of 20–45 m. The site of this input is near the continental shelf break off the South Carolina coast between 32°–33°N and 78.5°–79.5°W. Repeated transects over this area reveal enrichments of ^{226}Ra , ^{228}Ra , and Ba by factors of 3–4 above ambient ocean concentrations. The short-lived ^{223}Ra and ^{224}Ra are enriched by over an order of magnitude. The Ra and Ba enrichments are not caused by upwelling of deep water as no such ^{226}Ra or Ba concentrations occur in the upper 2000 m of the Atlantic Ocean. Sediments in the region are largely relic sand and do not offer a viable source for ^{226}Ra , ^{228}Ra , and Ba enrichments. We conclude that the source is the discharge of submarine fluids enriched in ^{226}Ra , ^{228}Ra , and Ba. The salinity of water in the Ra–Ba-enriched zone is diluted by 0.2–0.6‰ relative to water at the same depth farther offshore. Pronounced salinity and density anomalies characterize one site of active discharge. Estimates of ^{226}Ra and Ba concentrations in the fluids and the replacement time of water in the enriched zone suggest the fluid flux is similar to the summertime flow of major rivers in the area. The region of Ra–Ba enrichment is also characterized by a strong fluorescence signal, indicating high concentrations of chlorophyll in the water. It is probable that the leaking fluids supply nutrients that stimulate productivity in the bottom waters which are within the photic zone. Because the fluorescence signal is restricted to depths greater than 20 m, it is unlikely that the signal could be recognized by satellite or aircraft sensors.

1. Introduction

Mixing between meteoric water and seawater produces brackish to salty water in many coastal aquifers. In this mixing zone, chemical reactions of the salty water with aquifer solids modify the composition of the fluid; much as riverine particles and suspended sediments modify the composition of surface estuarine waters. The mixture is chemically distinct from either component because of the chemical reactions [Tsunogai *et al.*, 1996; Moore, 1996].

Advection of these modified fluids into the coastal ocean provides a potentially important source of some elements to the ocean. This source function is a product of the volume of fluid exchanging and the difference in concentration from the ambient coastal waters. Several studies demonstrate that these fluids are highly enriched in Ra, Rn, Ba, N, and P. For example, fluids entering the South Atlantic Bight contain at least 100 times more ^{226}Ra and 10 times more Ba than local rivers [Moore, 1996; Shaw *et al.*, 1998]. Salty groundwater sampled in the North Inlet, South Carolina, salt marsh contains up to 200 $\mu\text{M kg}^{-1}\text{ NH}_3$ and 10 $\mu\text{M kg}^{-1}\text{ PO}_4$ [Krest and Moore, 1996].

Because of the diffuse nature of subsurface fluid advection and the difficulty in recognizing and quantifying its importance, few investigators have attempted to assess the fluid flux and its impact on ocean chemistry and biology. Evidence is mounting that this source must be considered in the mass bal-

ance of some elements in the ocean [Moore, 1996; Church, 1996; Tsunogai *et al.*, 1996; Cable *et al.*, 1996; Shaw *et al.*, 1998]. The effect of fluid advection on coastal ocean productivity may be enormous in some regions [Johannes, 1980; Valiela *et al.*, 1990; Simmons, 1992].

Submarine fluid input is different from river input not only due to concentration differences but also because of the way it is added. Mixing of river water and seawater in particle-rich estuarine environments sequesters many of the trace elements and nutrients delivered by rivers through flocculation, adsorption, and intense biological productivity. Consequently, estuarine processes (rather than river water chemistry) determine the net flux of many elements to the coastal ocean via rivers. Because submarine fluids may bypass the biological components of the estuary filter, the elements delivered by this route are more likely to be mixed into the coastal and interior ocean rather than removed into estuarine and nearshore sediments. Thus the advection of submarine fluids represents an input flux of trace elements and nutrients for which the magnitudes and the chemical processes are virtually unknown.

In this study we document the input of submarine fluids below the pycnocline on the continental shelf through measurements of Ra and Ba tracers. We further attempt to estimate the fluid flux and composition required to balance the enrichments of ^{226}Ra , ^{228}Ra , and Ba.

2. Study Area

The continental shelf off South Carolina consists of a thick sequence of Tertiary limestone overlain by relic sand. Drilling has revealed that substantial fresh water lies trapped in these sediments. The AMCOR project [Hathaway *et al.*, 1979] drilled

Copyright 1998 by the American Geophysical Union.

Paper number 98JC02232
0148-0227/98/98JC-02232\$09.00

19 cores on the continental shelf from Cape Cod, Massachusetts, to northern Florida and noted that fresh or slightly brackish waters underlie much of the Atlantic continental shelf. JOIDES test hole J-1B drilled 40 km offshore from Jacksonville, Florida, tapped an aquifer that produced a flow of fresh water to an height of 10 m above sea level [Kohout *et al.*, 1988].

Offshore freshwater springs are noted still on nautical maps and are especially evident in karstic limestone off the Atlantic coast of Florida [Kohout *et al.*, 1977]. Barans and Henry [1984] describe the Charleston sink hole (Figure 1) approximately 34 km east southeast of Charleston at 42 m depth (32°32.5'N, 78°37.5'W). It was discovered by submersible as a 15 m diameter feature of unknown depth. The area around the sink hole is an old karst surface.

Samples reported in this paper were collected from the coastal ocean off South Carolina between August 13 and 19, 1995. During this cruise we sampled waters on the shelf along transects from the coast to the shelf break (Figure 1). The water column was characterized by a well mixed surface layer 15-20 m thick with temperature >28°C and salinity equal to 35.2-35.5‰. Between 20-45 m water depth, temperature decreased 1°-2°C and salinity increased 0.3‰ to form a homogenous bottom layer over most of the region. Samples collected just beyond the shelf break had higher salinity in the 20-45 m depth range, reaching 36.75‰ at 70 m depth. Such conditions typify water masses on the outer and middle shelf when Gulf Stream induced upwelling is minimal [Atkinson, 1985].

The conditions during August 1995 contrast sharply with an earlier study in July 1994. During the 1994 study [Moore, 1996; Moore *et al.*, 1998], the bottom water on the shelf was 8°-10°C colder than surface waters, and salinity was up to 1‰ higher. Such conditions represent strong Gulf Stream induced upwelling. We collected only a few bottom samples during the

1994 cruise and did not observe significant enrichments in ²²⁶Ra, ²²⁸Ra, and Ba below the surface layer.

3. Methods

At each station we first measured the structure of the water column using a conductivity-temperature-depth (CTD) with a Chelsea fluorometer. The fluorometer was set to monitor chlorophyll-a at an emission wavelength of 685 nm. After the CTD cast, we attached a hose to the CTD cage and redeployed the CTD to pump a large volume (200-400 L) sample into a drum on the R/V *Cape Hatteras*. A subsample from the drum was immediately passed through a 0.45 µm filter and reserved for Ba and U analyses. An unfiltered subsample was reserved for salinity measurement. These were measured at sea using a salinometer. The large volume samples were not filtered. The volume was recorded, and the water was pumped through a column of manganese-coated acrylic fiber (Mn-fiber) to quantitatively remove Ra [Moore, 1976].

The samples were measured at sea to determine activities of short-lived Ra isotopes, ²²⁴Ra (half-life equal to 3.6 days) and ²²³Ra (half-life equal to 11.4 days). Each Mn-fiber sample containing adsorbed Ra was partially dried by passing air down through a vertical tube containing the fiber for 15-30 min. Drying was stopped when no water droplets emerged after compressing the fiber bundle to the bottom of the drying tube and forcing air through it. The damp fiber was fluffed and placed in tube connected to a closed loop circulation system described by Moore and Arnold [1996]. The system was flushed with helium then closed. The helium was recirculated over the Mn-fiber to sweep the ²¹⁹Rn and ²²⁰Rn generated by ²²³Ra and ²²⁴Ra decay through a 1.1 L scintillation cell where alpha particles from the decay of Rn and daughters were recorded by a photomultiplier tube (PMT) attached to the scintillation cell.

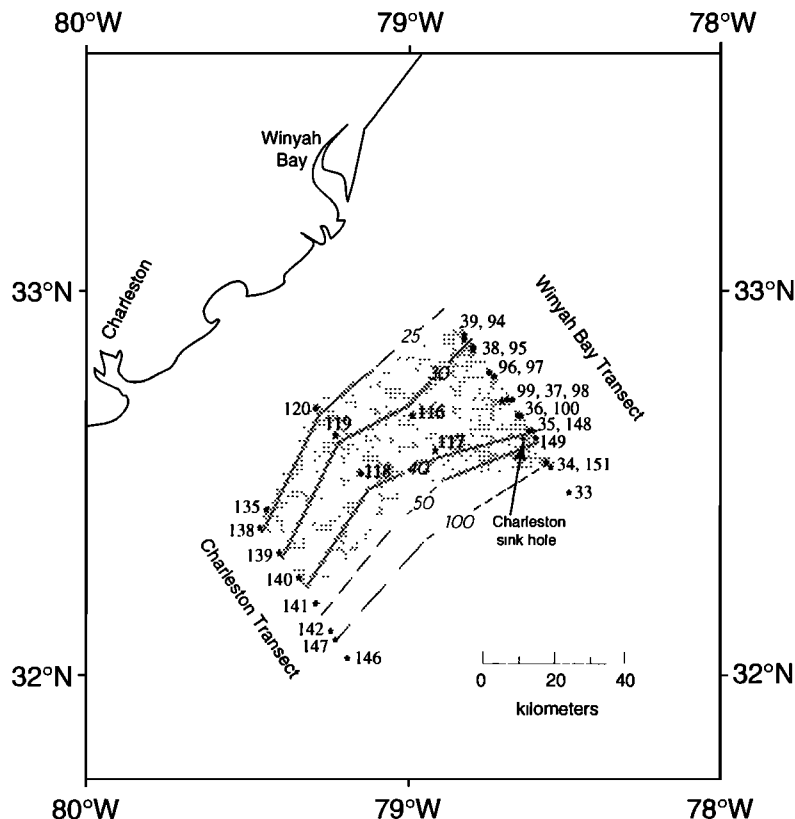


Figure 1. Map of the study area. Stations (asterisks) are indicated by numbers. Depth contours (m) are noted. The Charleston sink hole is described by Barans and Henry [1984].

Signals from the PMT were routed to a delayed coincidence system pioneered by *Giffin et al.* [1963] and adapted for Ra measurements by *Moore and Arnold* [1996]. The delayed coincidence system utilizes the difference in decay constants of the short-lived Po daughters of ^{219}Rn and ^{220}Rn to identify alpha particles derived from ^{219}Rn or ^{220}Rn decay and hence determine activities of ^{223}Ra and ^{224}Ra on the Mn-fiber. Most samples were counted initially for 10-60 min to measure ^{224}Ra and stored for 8-12 days. A second count of 1-10 hours provided a measure of ^{223}Ra . This procedure enabled a rapid assessment of Ra enrichment without building up excessive backgrounds of the ^{224}Ra daughter, ^{212}Pb , in the detector. The longer count for ^{223}Ra was made after much of the ^{224}Ra had decayed. The expected error for the ^{223}Ra and ^{224}Ra measurements is $\pm 10\%$.

After the ^{223}Ra and ^{224}Ra measurements were complete, the Mn-fiber samples were aged for 3-6 weeks to allow initial excess ^{224}Ra to equilibrate with ^{228}Th adsorbed to the Mn-fiber. The samples were measured again to determine ^{228}Th and correct for supported ^{224}Ra . Some samples were stored for 2 months to allow ^{223}Ra to equilibrate with ^{227}Ac . The activities of ^{227}Ac measured for these samples were not significantly above the detection limit, indicating that an insignificant fraction of the ^{223}Ra in bottom waters is supported by ^{227}Ac .

After the supported ^{224}Ra measurements were complete, Mn-fibers were leached with HCl in a Soxhlet extraction apparatus to quantitatively remove the long-lived Ra isotopes. The Ra was coprecipitated with BaSO_4 . The precipitant was aged 2 weeks to allow ^{222}Rn and its daughters to equilibrate with ^{226}Ra . The samples were measured in a gamma-ray spectrometer to assess the activities of ^{226}Ra and ^{228}Ra [*Moore, 1984; Moore et al., 1985*]. The expected error for the ^{226}Ra and ^{228}Ra measurements is $\pm 7\%$.

Approximately 18 months after collection, the Ba-U samples were acidified with nitric acid to dissolve any precipitated BaSO_4 through conversion of SO_4^{2-} to its acidified forms. After waiting several days to dissolve BaSO_4 that might have precipitated during storage, aliquots of the samples were diluted by a factor of 100 and spiked with ^{135}Ba and ^{236}U . These were analyzed using isotope dilution-inductively coupled plasma mass spectrometry (ICP-MS) on the Finnigan Element at the University of South Carolina following the Ba procedure of *Klinkhammer and Chan* [1990] and the U procedure of *Klinkhammer and Palmer* [1991]. The expected error for the Ba and U measurements is $\pm 5\%$.

4. Results

Table 1 gives the Ra isotope, Ba, and U data for samples collected in the area outlined in Figure 1. Figure 2 shows a ^{226}Ra section along a transect extending from the mouth of Winyah Bay, South Carolina, to the edge of the continental shelf. There are two regions of ^{226}Ra enrichment, near the coast in 10-15 m water depths and 40-80 km offshore in 25-45 m water depths. The other Ra isotopes and Ba are also enriched in these two regions. The deep samples enriched in Ra and Ba are shown by asterisks in Table 1. Here we define the deep enriched samples as those >15 m deep with ^{226}Ra >9 dpm 100 L^{-1} compared to the open ocean activity of 7.5 dpm 100 L^{-1} . The mean ^{226}Ra activity in the enriched zone is 17.5 dpm 100 L^{-1} . We note that a few samples having highest ^{226}Ra enrichments are not proportionately enriched in Ba (e.g. G35-33, G99-26, G100-26). Whether this is due to a divergence in Ba and Ra behavior or the failure of our technique to redissolve all of the Ba that may have precipitated is unknown. Uranium concentration ($14.7 \pm 0.4\text{ nM kg}^{-1}$) is not significantly different from salinity-adjusted seawater U concentrations in these samples; U concentration does not correlate with Ra or Ba.

The nearshore, shallow water enrichments (Figure 2) are similar to results obtained in July 1994. In this earlier study, *Moore* [1996] and *Shaw et al.* [1998] demonstrated that nearshore ^{226}Ra and Ba enrichments were derived from the input of subsurface fluids along the coast. In this paper we shall focus on the sites of deeper ^{226}Ra and Ba enrichment, 40-80 km offshore.

The deep offshore Ra-Ba-enriched zone extended at least 80 km along the shelf and covered an area of 2600 km^2 . During the 1995 cruise extensive bottom water samples of the outer shelf were obtained between the Winyah Bay and Charleston transects (Figure 1). In this region the average thickness of the deep enriched zone was 15 m, therefore the volume was $4 \times 10^{10}\text{ m}^3$. The ^{226}Ra activity within the enriched zone averaged 10 dpm 100 L^{-1} greater than surrounding ocean water (Table 1, samples with asterisks) to yield a total ^{226}Ra enrichment of 4×10^{12} dpm. The average Ba enrichment was 60 nM kg^{-1} greater than surface ocean water (Table 1, samples with asterisks) for a total Ba enrichment of 2.4×10^6 moles.

Coincident with the enrichments in Ra and Ba in the bottom waters are elevated concentrations of chlorophyll-a as determined from in situ fluorescence measurements at an emission

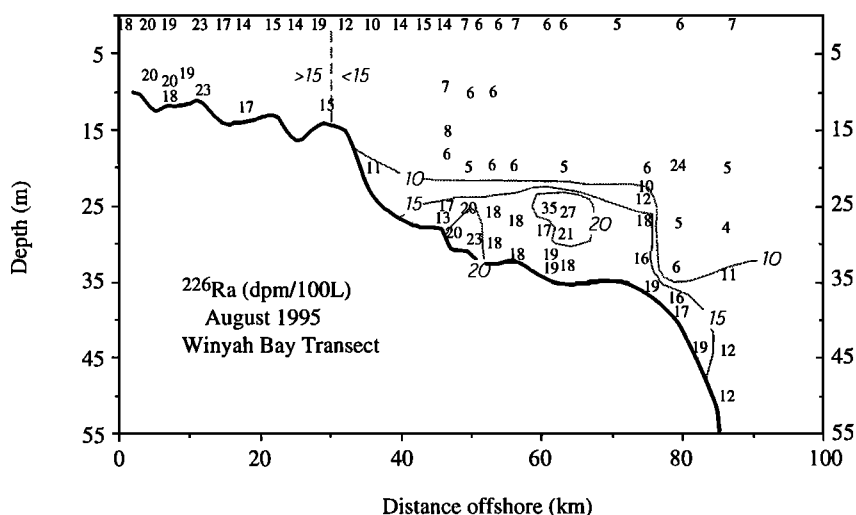


Figure 2. Cross section of ^{226}Ra (dpm 100 L^{-1}) along the Winyah Bay transect.

Table 1. Ra, Ba, and U Data for Middle and Outer Shelf Stations

| Sample | Depth m | Salinity ‰ | Temperature °C | Fluorescence V | U | Ba | ²²⁶ Ra | ²²⁸ Ra | ²²³ Ra | ex ²²⁴ Ra |
|----------|------------|---------------|-------------------|-------------------|-------|--------|-------------------|-------------------|-------------------|----------------------|
| G33-2 | 2 | 35.668 | 29.3 | 0.04 | 14.7 | 37.4 | 5.63 | 5.24 | 0.11 | -0.13 |
| G34-2 | 2 | 35.731 | 28.8 | 0.04 | 14.6 | 47.5 | 7.49 | 6.83 | 0.16 | 0.55 |
| G35-2 | 2 | 35.654 | 28.5 | 0.04 | | | 6.41 | 5.88 | 0.13 | 0.94 |
| G35-20 | 20 | 35.662 | 28.3 | 0.04 | | 48.0 | 5.71 | 4.87 | 0.50 | 6.03 |
| G35-33* | 33* | 36.050* | 25.1* | 0.08* | | 45.3* | 25.18* | 25.17* | 0.92* | 2.21* |
| G35-39* | 39* | 36.200* | 24.8* | 0.38* | | 90.3* | 16.89* | 13.93* | 2.30* | 7.96* |
| G36-2 | 2 | 35.570 | 28.5 | 0.05 | | | 5.44 | 6.26 | 0.29 | 0.52 |
| G37-2 | 2 | 35.388 | 28.5 | 0.06 | | | 6.07 | 7.03 | 0.48 | 1.15 |
| G37-32* | 32* | 35.904* | 25.8* | 0.38* | | 180.8* | 18.78* | 20.88* | 3.10* | 10.50* |
| G38-2 | 2 | 35.317 | 28.5 | 0.08 | 14.5 | 34.7 | 6.29 | 6.99 | 0.44 | 1.21 |
| G38-13 | 13 | 35.436 | 28.3 | 0.09 | 13.8 | 41.1 | | | | |
| G39-2 | 2 | 35.284 | 28.5 | 0.10 | | | 6.65 | 8.12 | 0.81 | 5.39 |
| G39-15 | 15 | 35.299 | 28.2 | 0.10 | | 48.3 | 8.07 | 10.56 | 0.60 | 1.64 |
| G39-26* | 26* | 35.541* | 27.4* | 0.30* | | 102.2* | 13.04* | 15.42* | 2.18* | 7.06* |
| G94-2 | 2 | 35.317 | 28.5 | 0.08 | | 43.5 | 6.80 | 7.26 | 0.28 | 0.48 |
| G94-9 | 9 | 35.320 | 28.5 | 0.09 | | 65.2 | 7.01 | 7.76 | 0.47 | 1.18 |
| G94-18 | 18 | 35.324 | 28.5 | 0.09 | | | 6.48 | 7.36 | 0.64 | 1.88 |
| G94-25* | 25* | 35.455* | 27.7* | 0.35* | | 84.4* | 16.93* | 19.29* | 2.82* | 11.27* |
| G94-29* | 29* | 35.516* | 27.5* | 0.55* | | 101.6* | 20.01* | 21.83* | 1.64* | 11.06* |
| G95-2 | 2 | 35.317 | 28.5 | 0.09 | | | 6.93 | 9.37 | 0.33 | 1.21 |
| G95-10 | 10 | 35.315 | 28.5 | 0.09 | | 32.6 | 6.22 | 6.65 | 0.58 | 1.50 |
| G95-20 | 20 | 35.324 | 28.5 | 0.08 | | 46.4 | 5.43 | 6.70 | 0.39 | 0.81 |
| G95-25* | 25* | 35.579* | 27.2* | 0.50* | | 103.4* | 20.14* | 23.14* | 3.09* | 12.90* |
| G95-29* | 29* | 35.579* | 27.2* | 0.60* | | 98.4* | 22.90* | 26.17* | 3.48* | 16.94* |
| G96-2 | 2 | 35.361 | 28.4 | 0.07 | | 29.5 | 5.47 | 6.82 | 0.26 | 0.34 |
| G96-10 | 10 | 35.355 | 28.4 | 0.08 | | 33.6 | 5.87 | 7.60 | 0.37 | 0.86 |
| G96-20 | 20 | 35.355 | 28.4 | 0.08 | | 30.8 | 5.82 | 6.49 | 0.38 | 0.70 |
| G96-26* | 26* | 35.674* | 26.9* | 0.40* | | 91.9* | 17.64* | 18.92* | 2.08* | 8.74* |
| G96-30* | 30* | 35.702* | 26.9* | 0.58* | | 130.5* | 18.24* | 18.30* | 2.23* | 10.97* |
| G97-2 | 2 | 35.424 | 28.3 | 0.07 | | 32.9 | 6.59 | 6.75 | 0.28 | 0.57 |
| G97-20 | 20 | 35.417 | 28.3 | 0.08 | | 31.8 | 6.18 | 6.34 | 0.22 | 1.27 |
| G97-27* | 27* | 35.759* | 26.6* | 0.57* | | 107.6* | 18.41* | 19.57* | 3.97* | 16.41* |
| G97-32* | 32* | 35.785* | 26.6* | 0.60* | | 119.3* | 17.88* | 18.36* | 4.85* | 22.27* |
| G98-2 | 2 | 35.500 | 28.3 | 0.06 | 14.5 | 37.3 | | | | |
| G98-28* | 28* | 35.856* | 26.4* | 0.58* | | 131.8* | 16.47* | 16.30* | 4.68* | 15.38* |
| G98-33* | 33* | 35.844* | 26.4* | 0.63* | | 113.5* | 18.05* | 18.31* | 5.10* | 17.11* |
| G99-26* | 26* | 35.828* | 26.4* | 0.62* | | 97.0* | 34.93* | 40.34* | 4.12* | 20.69* |
| G100-2 | 2 | 35.570 | 28.2 | 0.05 | | 37.4 | 6.23 | 6.95 | 0.32 | 0.76 |
| G100-20 | 20 | 35.895 | 28.2 | 0.06 | | | 5.39 | 5.98 | 0.26 | 0.40 |
| G100-26* | 26* | 35.906* | 26.2* | 0.25* | | 87.1* | 26.75* | 28.29* | 3.95* | 19.16* |
| G100-29* | 29 | 35.909* | 26.2* | 0.57* | | 102.7* | 20.94* | 20.87* | 4.87* | 12.97* |
| G100-33* | 33* | 35.910* | 26.2* | 0.60* | | 98.4* | 18.90* | 19.75* | 5.05* | 17.75* |
| G116-2 | 2 | 35.530 | 28.5 | 0.06 | 14.6 | 43.4 | 5.96 | 6.57 | 0.44 | 1.24 |
| G116-21* | 21* | 35.644* | 27.8* | 0.20* | 14.5* | 85.7* | 14.40* | 13.87* | 1.01* | 5.39* |
| G116-30* | 30* | 35.671* | 27.9* | 0.32* | 14.5* | 96.7* | 15.38* | 14.62* | 1.61* | 13.45* |
| G117-2 | 2 | 35.728 | | | 15.0 | 39.2 | 5.92 | 4.70 | 0.23 | 0.28 |
| G117-30* | 30* | 35.980* | | | 15.0* | 114.0* | 15.76* | 20.03* | 2.50* | 8.60* |
| G117-36* | 36* | 35.989* | | | | | 16.73* | 14.59* | 2.67* | 12.23* |
| G118-2 | 2 | 35.426 | 28.5 | 0.05 | 14.5 | 35.1 | 5.77 | 5.77 | 0.19 | 0.24 |
| G118-18 | 18 | 35.754 | 28.5 | 0.05 | 14.8 | 43.3 | 6.75 | 5.87 | 0.14 | 0.20 |
| G118-30* | 30* | 35.956* | 26.7* | 0.15* | 14.7* | 84.8* | 15.58* | 14.22* | 2.88* | 14.27* |
| G118-39* | 39* | 36.040* | 26.2* | 0.37* | 15.0* | 97.6* | 16.02* | 13.10* | 1.76* | 12.26* |
| G119-2 | 2 | 35.513 | 28.5 | 0.05 | | | 5.34 | 5.88 | 0.44 | 0.88 |
| G119-13 | 13 | 35.543 | 28.5 | 0.05 | 14.7 | 38.8 | 5.47 | 6.18 | 0.23 | 0.68 |
| G119-18* | 18* | 35.758* | 27.5* | 0.18* | 14.8* | 86.6* | 11.39* | 13.15* | 2.34* | 7.46* |
| G119-25* | 25* | 35.799* | 27.5* | 0.27* | 14.9* | 94.3* | 14.88* | 15.27* | 2.02* | 8.22* |
| G120-2 | 2 | 35.159 | 28.4 | 0.14 | 14.5 | 52.6 | 7.20 | 8.99 | 0.28 | 0.68 |
| G120-23* | 23* | 35.466* | 28.1* | 0.26* | 14.6* | 71.6* | 11.67* | 13.37* | 0.98* | 6.51* |
| G135-2 | 2 | 35.274 | 28.7 | 0.13 | 14.2 | 71.7 | 9.90 | 13.26 | 1.18 | 3.22 |
| G135-7* | 7* | 35.290* | 28.7* | 0.11* | 14.4* | 76.6* | 11.90* | 16.68* | 1.46* | 2.98* |
| G135-14* | 14* | 35.321* | 28.4* | 0.19* | 14.4* | 124.5* | 11.59* | 15.92* | 1.49* | 4.28* |
| G135-19* | 19* | 35.318* | 28.4* | 0.20* | 14.6* | 95.4* | 14.05* | 18.53* | 1.15* | 3.59* |
| G139-2 | 2 | 35.474 | 28.8 | 0.08 | 14.7 | 50.7 | 7.53 | 10.00 | 0.86 | 2.10 |
| G139-13 | 13 | 35.489 | 28.7 | 0.08 | | | 6.40 | 6.83 | 0.80 | 1.40 |
| G139-20* | 20* | 35.663* | 27.5* | 0.30* | 14.3* | 119.4* | 15.41* | 16.10* | 2.10* | 7.04* |
| G139-28* | 28* | 35.693* | 27.3* | 0.43* | 14.7* | 118.6* | 18.40* | 19.26* | 1.97* | 7.97* |
| G140-2 | 2 | 35.409 | 28.7 | 0.07 | 14.4 | 48.4 | 6.25 | 7.71 | 0.58 | 1.11 |
| G140-10 | 10 | 35.420 | 28.7 | 0.07 | 14.7 | 43.2 | 6.19 | 5.81 | 0.64 | 1.61 |
| G140-25* | 25* | 35.796* | 27.2* | 0.42* | 15.4* | 95.7* | 13.65* | 13.00* | 1.65* | 6.24* |
| G140-38* | 38* | 35.814* | 27.2* | 0.43* | 15.3* | 101.0* | 16.36* | 15.66* | 1.60* | 9.79* |
| G141-2 | 2 | 35.650 | 28.8 | 0.06 | 14.7 | 35.9 | 5.50 | 5.51 | 0.33 | 0.18 |
| G141-15 | 15 | 35.702 | 28.7 | 0.07 | 14.9 | 47.4 | 7.51 | 7.10 | 0.57 | 0.71 |
| G141-28 | 28 | 35.991 | 28.3 | 0.09 | 15.2 | 58.4 | 7.71 | 4.82 | 0.75 | 3.10 |
| G141-45 | 45 | 36.096 | 27.2 | 0.25 | 15.7 | 66.2 | 8.45 | 6.08 | 0.94 | 7.17 |
| G142-2 | 2 | 36.030 | 29.4 | 0.04 | 15.4 | 56.6 | 6.78 | 3.99 | 0.07 | -0.01 |
| G142-25 | | 36.031 | 29.4 | 0.03 | 15.5 | 58.3 | 7.15 | 4.47 | | |
| G142-42 | 42 | 36.015 | 29.2 | 0.02 | 15.0 | 57.1 | 6.65 | 3.69 | 0.03 | 0.27 |
| G142-52 | 52 | 36.165 | 28.9 | 0.03 | 15.1 | 61.9 | | | 0.07 | 1.54 |
| G142-63 | 63 | 36.239 | 27.8 | 0.05 | 15.0 | 58.6 | 7.51 | 4.63 | 0.09 | 0.44 |
| G142-71 | 71 | 36.324 | 26.1 | 0.10 | | | 7.37 | 3.14 | 0.22 | 2.08 |
| G143-2 | 2 | 36.057 | 29.5 | 0.04 | | | 7.01 | 3.83 | 0.03 | 0.09 |
| G144-2 | 2 | 36.055 | 29.5 | 0.03 | | | 6.80 | 3.83 | 0.03 | 0.00 |

Table 1. (continued)

| Sample | Depth m | Salinity ‰ | Temperature °C | Fluorescence V | U | Ba | ²²⁶ Ra | ²²⁸ Ra | ²²³ Ra | ex ²²⁶ Ra |
|----------|------------|---------------|-------------------|-------------------|---|----|-------------------|-------------------|-------------------|----------------------|
| G146-2 | 2 | 35.926 | 29.5 | 0.04 | | | 7.82 | 4.84 | 0.02 | 0.32 |
| G146-35* | 35* | 36.063* | 28.6* | 0.06* | | | 9.56* | 4.81* | 0.08* | 0.58* |
| G146-46 | 46 | 36.333 | 26.1 | 0.15 | | | 7.41 | 3.41 | 0.05 | 0.84 |
| G146-66 | 66 | 36.633 | 23.2 | 0.07 | | | 6.59 | 2.50 | 0.01 | 0.47 |
| G146-80 | 80 | 36.682 | 22.0 | 0.04 | | | 7.29 | 1.70 | 0.02 | 0.47 |
| G146-90 | 90 | 36.737 | 21.1 | 0.03 | | | 6.89 | 2.22 | 0.02 | 0.49 |
| G146-101 | 101 | 36.620 | 19.5 | 0.04 | | | 7.28 | 1.91 | 0.04 | 0.32 |
| G146-114 | 114 | 36.396 | 18.2 | 0.04 | | | 7.19 | 1.04 | 0.06 | 0.83 |
| G147-38 | 38 | 36.074 | 27.9 | 0.05 | | | 7.23 | 4.63 | 0.04 | 0.86 |
| G147-50 | 50 | 36.415 | 24.7 | 0.15 | | | 5.92 | 2.75 | 0.05 | 0.40 |
| G147-63 | 63 | 36.610 | 24.3 | 0.08 | | | 7.13 | 2.91 | 0.04 | 0.19 |
| G147-71 | 71 | 36.751 | 23.5 | 0.06 | | | 6.63 | 1.84 | 0.03 | 0.53 |
| G148-20 | 20 | 35.697 | 28.5 | 0.07 | | | 6.04 | 5.57 | 0.64 | 1.48 |
| G148-22* | 22* | 35.794* | 27.2* | 0.08* | | | 9.61* | 10.77* | 1.81* | 3.89* |
| G148-24* | 24* | 35.769* | 26.7* | 0.24* | | | 11.70* | 12.06* | 1.75* | 6.47* |
| G148-27* | 27* | 35.808* | 26.5* | 0.44* | | | 18.17* | 20.06* | 3.57* | 9.06* |
| G148-32* | 32* | 35.717* | 26.5* | 0.48* | | | 16.50* | 16.79* | 2.72* | 8.06* |
| G148-37* | 37* | 35.828* | 26.4* | 0.48* | | | 18.96* | 20.77* | 4.35* | 11.36* |
| G149-27 | 27 | 35.660 | 28.8 | 0.08 | | | 4.93 | 5.92 | 0.33 | 0.93 |
| G149-37* | 37* | 35.875* | 26.3* | 0.54* | | | 15.83* | 18.75* | 3.15* | 7.44* |
| G149-44* | 44* | 35.897* | 26.2* | 0.54* | | | 18.85* | 18.82* | 4.02* | 8.94* |
| G151-20 | 20 | 35.543 | 28.5 | 0.07 | | | 5.23 | 6.97 | 0.52 | 3.08 |
| G151-28 | 28 | 35.589 | 28.3 | 0.05 | | | 4.31 | 5.36 | 0.34 | 0.56 |
| G151-34* | 34* | 35.473* | 27.5* | 0.10* | | | 11.20* | 16.43* | 2.45* | 6.51* |
| G151-44* | 44* | 35.978* | 26.0* | 0.59* | | | 11.49* | 17.23* | 3.17* | 9.16* |
| G151-50* | 50* | 35.997* | 26.0* | 0.53* | | | 12.48* | 16.36* | 2.62* | 6.37* |
| G151-58* | 58* | 35.984* | 26.0* | 0.48* | | | 16.51* | 19.04* | 2.98* | 8.38* |
| G151-64* | 64* | 36.012* | 25.8* | 0.47* | | | 11.97* | 16.23* | 2.87* | 9.33* |
| G151-68* | 68* | 36.015* | 25.8* | 0.47* | | | 15.72* | 18.50* | 3.32* | 10.50* |

Ra data are dpm 100 L⁻¹. Ba and U are nM kg⁻¹.

*Samples containing significant enrichments in Ra and Ba

wavelength of 685 nm. Some large volume water samples pumped from depth had a scum of green pigments on the surface. Stations farther offshore on the Charleston transect which did not have enrichments in Ra and Ba had much lower fluorescence signals in the bottom water. Figure 3 shows the CTD-fluorometer cast for Station 100 on the Winyah Bay transect in the region of deep Ra enrichment. This cast is typical of most casts in this depth range. The bottom 5 m of the water column contains a water mass with temperature about 2°C colder and 0.3‰ more salty than surface waters. This bottom water has a fluorescence signal 10 times greater than the surface water. Figure 4 is a cross section of fluorescence for the region covered in Figure 2. The highest fluorescence readings are within 5 m of the bottom in water depths of 30-35 m. Elevated readings extended 10-12 m above the bottom.

At one station on the Winyah Bay transect (station G98), we noted a lens of warm (26.5°C), high salinity (36.8‰) water at 25 m depth overlying water of lower salinity (36.3‰). Three CTD casts into this salty layer confirmed its presence. Figure 5 is a temperature-salinity plot of the CTD data from station 98 compared to station 99, which was typical of other stations on the transect. After confirming its presence, we attempted to pump a large volume sample from the high-salinity layer at station 98. Normally, we did not record the CTD output during the pumping casts; but, because this was the first time we had encountered a high-salinity layer on the Winyah Bay transect, we recorded the entire pumping cast. The CTD was positioned near 25 m depth in the high-salinity layer as we began to pump a 200 L sample, but then the salinity abruptly decreased. We attempted to relocate the high-salinity layer but could not position the CTD in it long enough to pump a sample. After several attempts, we lost all traces of the high-salinity layer. The CTD record later revealed that during the search, salinity suddenly dropped from >36 to 35.1‰ and then increased to 35.8‰ as the CTD was lowered from 25 to 33 m. The low-salinity readings do not appear to be a malfunction of the CTD as they follow a consistent trend along a T-S mixing

line (Figure 5, third cast lower). We suspect the freshened water recorded during this cast, but not sampled, represents a plume of low-salinity fluid mixing with seawater. The source of the high-salinity plume is uncertain. No other water with these T-S characteristics were encountered on the cruise.

Each of the CTD casts at station 98 revealed a layer of lower density ($\sigma_t < 23.9$) water underlying the high-salinity layer of $\sigma_t > 24.2$ (Figure 6). The density inversion was present on each

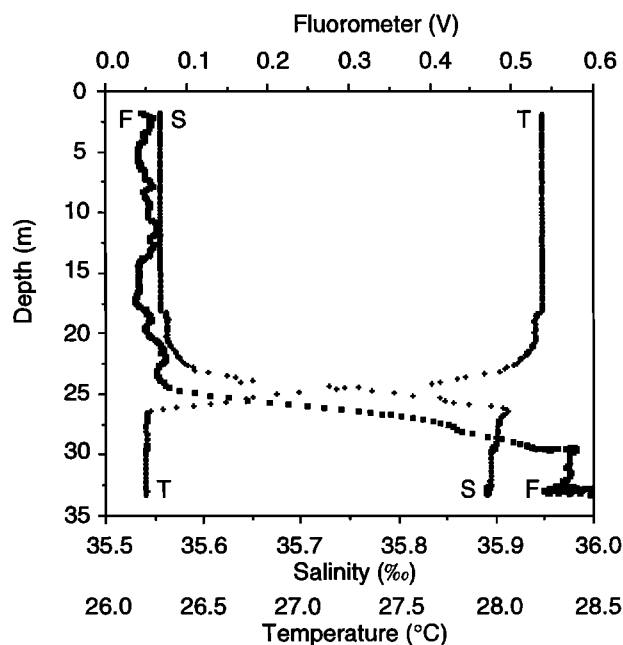


Figure 3. Temperature, salinity, and fluorescence with depth at station G100 on the Winyah Bay transect.

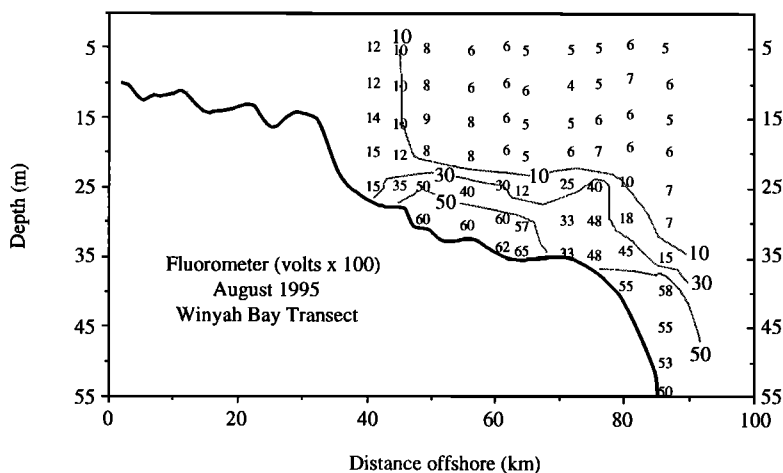


Figure 4. Cross section of chlorophyll-a fluorescence as determined at an emission wavelength of 685 nm along the Winyah Bay transect. The values are plotted as volts x 100.

of the three casts at this station and clearly represents an unstable structure, probably resulting from the advection of a low-salinity fluid.

5. Discussion

5.1. What is the Source of the Ra and Ba Enrichment?

Upwelling of deep water, induced by Gulf Stream meanders, can supply nutrients to waters on the continental shelf [Atkinson, 1985]. However, the water in the Ra-Ba-enriched zone was only 1°-2°C cooler than surface waters. The water in the enriched zone did not result from deep upwelling. Further-

more, upwelling of deeper water cannot supply the enrichments of ^{226}Ra , ^{228}Ra , and Ba measured during this investigation. Key *et al.* [1985] have mapped distributions of ^{226}Ra and ^{228}Ra in the Atlantic Ocean as part of the Transient Tracers in the Ocean (TTO) and Western Boundary Exchange Experiment (WEBEX) programs. The results from these extensive studies corroborate earlier Geochemical Oceans Sections Study (GEOSECS) data [Oslund *et al.*, 1987] that no activities of ^{226}Ra in the upper 2000 m of the open North Atlantic exceed 12 dpm 100 L^{-1} , and nowhere in the Atlantic do open ocean activities exceed 20 dpm 100 L^{-1} . Similar arguments can be made for Ba; no GEOSECS samples from the upper 2000 m in the North Atlantic exceed 62 nM kg^{-1} [Chan *et al.*, 1977]. Therefore the ^{226}Ra and Ba enrichments measured on the continental shelf (Table 1, Figure 2) cannot result from upwelling of deeper waters. For the ^{228}Ra enrichments the case is even stronger; $^{228}\text{Ra}/^{226}\text{Ra}$ activity ratios (ARs) normally decrease with depth through the thermocline, yet the zone of Ra enrichment has $^{228}\text{Ra}/^{226}\text{Ra}$ ARs >1. Figure 7 is a summary of ^{226}Ra and ^{228}Ra data from the regions of Ra enrichment and from samples col-

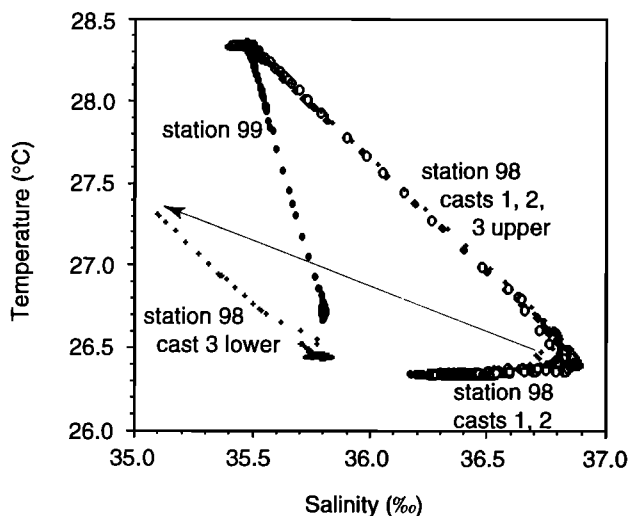


Figure 5. Temperature-salinity plots for stations 98 and 99. The data from station 99 are typical of other stations on the Winyah Bay transect. Three casts at station 98 revealed a high-salinity layer at 25 m depth (noted as station 98, casts 1, 2, 3 upper) overlying lower-salinity water (noted as station 98, casts 1, 2). As we attempted to sample this high-salinity layer during cast 3, we encountered a low-salinity lens (designated station 98, cast 3 lower). The arrow shows the displacement of the T-S record from the high-salinity layer to the fresher water during cast 3. Cast 3 ended in water of similar composition to the bottom water at station 99.

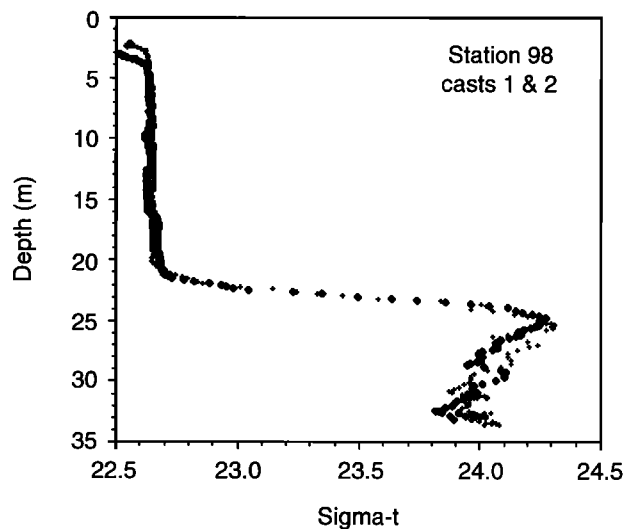


Figure 6. The density of the water underlying the high-salinity layer at station 98 is lower by up to 0.5 sigma-t units. This density inversion must be caused by the injection of low-salinity water at the sea bed.

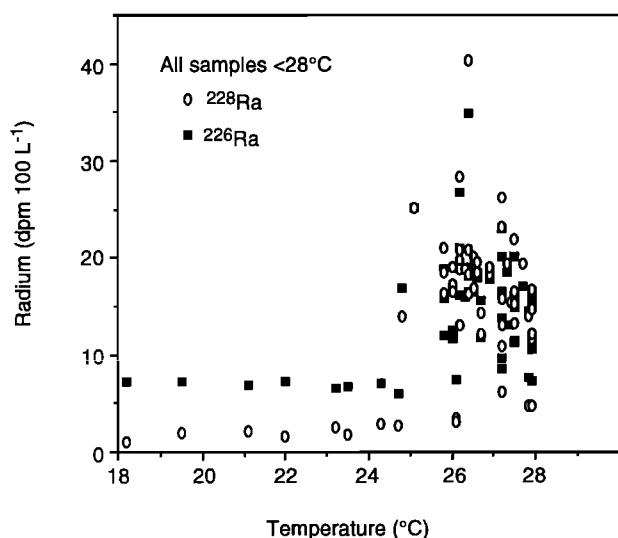


Figure 7. The ^{226}Ra and ^{228}Ra versus temperature for samples on the outer shelf with $t < 28^\circ\text{C}$.

lected near the shelf break to 120 m water depth. These samples show strong Ra enrichments for most samples in the temperature range $24.8^\circ\text{--}27.9^\circ\text{C}$, but no Ra enrichment for deeper samples with temperatures in the range $18.2^\circ\text{--}24.7^\circ\text{C}$; in fact for samples $< 24.7^\circ\text{C}$, ^{226}Ra activities are similar to surface values, and ^{228}Ra activities are considerably lower. Upwelling of deep water is not the source of the ^{226}Ra , ^{228}Ra , or Ba enrichment.

Sediments in this region are largely relic sands and gravel with some shell, coral, and phosphorite fragments. They are not expected to be a viable source for the Ra or Ba enrichment. On the basis of direct gamma measurements of grab samples, most sediments have low concentrations of ^{226}Ra and ^{228}Ra . The exception is samples containing phosphorite. Could the ^{226}Ra enrichment be derived from phosphorite dissolution? Evidence from ^{228}Ra suggests this is not the case. Figure 8 shows that the water samples enriched in ^{226}Ra are even more enriched in ^{228}Ra . However, ^{232}Th is not enriched in phosphorite, and the $^{228}\text{Ra}/^{226}\text{Ra}$ AR in the phosphorite is < 0.01 (as measured by direct gamma ray spectrometry). The high correlation between ^{228}Ra and ^{226}Ra (Figure 8) is compelling evidence that these isotopes derive from the same source, which cannot be phosphorite. Furthermore, the ^{226}Ra enrichments in the water are not correlated with higher U concentrations. If the source of ^{226}Ra was phosphorite dissolution, we would expect to also measure U enrichments.

Having eliminated surficial sediments and deeper water, the most probable remaining source for the ^{226}Ra , ^{228}Ra , and Ba enrichment is direct injection of subsurface fluids enriched in Ra and Ba and depleted in salt. This source explains the enriched Ra and Ba and the freshened deep water. Earlier studies have demonstrated fluid advection to be the primary source for ^{226}Ra , ^{228}Ra , and Ba enrichments in salt marshes and on the inner shelf [Rama and Moore, 1996; Moore, 1996; Cable et al., 1996; Shaw et al., 1998]. The results of this study lead to the conclusion that fluid injection also occurs far from shore.

The zone of ^{226}Ra , ^{228}Ra , and Ba enrichment also contains high activities of ^{223}Ra and ^{224}Ra compared to open ocean water. Because of the rate at which they are regenerated on sediments, the potential sources of the short-lived Ra isotopes are more complex. For example, the enrichments of ^{223}Ra could result from the injection of ^{227}Ac into the deep water followed by the rapid removal of its daughter, ^{227}Th , to the sediments and the subsequent release of ^{223}Ra . However, our attempted meas-

urements of ^{227}Ac in the deep water found activities near the lower limit of detection, ~ 0.1 dpm 100 L^{-1} . The lack of ^{227}Ac enrichment means the ^{223}Ra enrichments must also derive from fluid advection. For ^{224}Ra we could construct a similar scenario based on the scavenging of ^{228}Th after its production by ^{228}Ra decay followed by the release of ^{224}Ra from the sediments. However, the sediments are not significantly enriched in ^{228}Th ; therefore we conclude the ^{224}Ra must also derive from subsurface fluid injection.

5.2. What is the Flux of Ra and Ba Required to Produce the Enrichments?

The deep zone of Ra and Ba enrichment is probably a transient feature. Enrichments of Ra and Ba in this region were not detected in July 1994 when upwelling of deeper waters onto the shelf was prominent. During 1994, deep sampling was limited, and we may have missed the signal. However, we suspect that upwelling events strongly dilute the signal derived from advecting fluids. If this is true, we should only be able to detect the signal during a time when the water on the shelf is not rapidly exchanged.

To estimate Ra and Ba fluxes, we must know the length of time available to accumulate the enrichment. The enriched zone extended from the middle to the outer shelf, a region strongly affected by the Gulf Stream. Atkinson and Menzel [1985] note that during the summer, currents on the outer shelf generally range from $30\text{--}40\text{ cm s}^{-1}$, but are variable. A 30 cm s^{-1} longshore current could sweep all of the water from the enriched zone in 3 days. On the other hand, a 5 cm s^{-1} current, more typical of the middle shelf, would take 20 days to remove it. The water could also be replaced by periodic upwelling at the shelf break. Atkinson [1985] and Yoder [1985] estimated that upwelling events on the outer shelf caused by Gulf Stream frontal eddies occur every 2-14 days throughout the year. During the summer, some of these events may penetrate to the midshelf. We sampled the enriched zone three times between August 13 and 19. The long- and short-lived Ra isotopes were all enriched each time we sampled. Although each sampling recorded some high and some low activities, in general the activity ratios of the short- to long-lived Ra isotopes were similar. On August 13 the average $^{224}\text{Ra}/^{226}\text{Ra}$ AR was 0.4; on August 16-17 it was 0.7, and on August 19 it was 0.5. Since the sampling extended over two ^{224}Ra half-lives, we would expect the

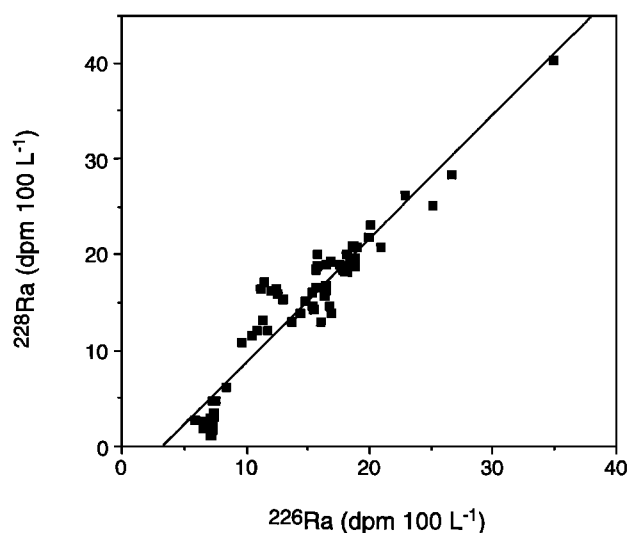


Figure 8. A high correlation ($R^2 = 0.90$) of the activity of ^{228}Ra versus ^{226}Ra demonstrates they have similar sources on the outer shelf.

AR to decrease unless the ^{224}Ra activity was being continuously replaced. For $^{223}\text{Ra}/^{226}\text{Ra}$ the average ARs for the same periods were 0.12, 0.17, and 0.17. Again, no sign of decay is evident. To maintain a fairly constant ratio of the short-/long-lived Ra isotopes, the water in the enriched zone must be replaced on a timescale of ~ 10 days. On the basis of the physical and radiochemical evidence we conservatively estimate replacement times for water in the enriched zone in the range 10–20 days.

The following mass balance equation may be used to estimate the average flux required to produce the enrichment. We will express this flux on a per day basis, but we realize that it need not be a steady source. We assume that water in the enriched zone is a mixture of fluids entering from below and water from further offshore having activities of Ra and Ba typical of open ocean water.

$$\frac{V_E}{T} = \frac{Q_f C_f}{C_E - C_0} \quad (1)$$

where V_E is volume of the enriched zone; T is replacement time; Q_f is flux of subsurface fluid into the enriched zone; C_f is Ra concentration in the fluid; C_E is Ra concentration in the enriched zone; and C_0 is Ra concentration in the adjacent ocean.

Table 2 gives the ^{226}Ra , ^{228}Ra , and Ba fluxes required to produce the concentrations in the enriched zone for 10 and 20 day replacement times. The required ^{226}Ra flux to the deep shelf is 2.4×10^{11} dpm d^{-1} , a value similar to the flux to the entire 320 km long inner shelf calculated by Moore [1996].

To separate the two factors controlling this deep flux, Q_f and C_f , estimates of the ^{226}Ra activity of the fluid are required. We have measured ^{226}Ra in numerous high-salinity groundwaters from limestone aquifers that we think are equivalent to the aquifers underlying the shelf. In no case has the ^{226}Ra activity exceeded 12 dpm L^{-1} ; most values are in the range 2–8 dpm L^{-1} . If the fluid has a ^{226}Ra activity in this range, the fluid flux must be of the order of 300–2000 $\text{m}^3 \text{s}^{-1}$ from this 80 km long segment of the outer shelf. The concentrations of Ba in the high-salinity groundwater are in the range 300–3000 nM kg^{-1} . If fluids of this concentration are causing the Ba anomaly, a fluid flux of 500–9000 $\text{m}^3 \text{s}^{-1}$ would be required. Although there is considerable spread in these estimates, it is clear that substantial volumes of submarine fluid input are required. To put these fluid fluxes into perspective, the lowest estimates are similar to the average flow of the Savannah or Pee Dee River. We caution that these fluid fluxes are based on assumed concentrations of the tracers in the fluids and are calculated for one period of enrichment only. Further data on the fluids and more studies of outer shelf waters are required to evaluate total annual fluxes.

5.3. Salt Balance in the Ra-Enriched Zone

The three CTD casts from station 98 each revealed a density inversion in the lower 8 m of the water column (Figure 6). This could only result from input of fresher water at the seabed. The pumping cast from this station apparently recorded a plume of the fresher water as it was mixing with the ambient water (Figure 5). However, because the unstable density structure drives rapid mixing, it is not possible to derive the flux of fresh water from a few CTD profiles. Instead, we will use ^{226}Ra

as a tracer of water that has been added by fluid advection to estimate the salt balance.

Figure 9a shows the distribution of ^{226}Ra with depth for representative stations. Stations having some samples with Ra enrichments are indicated by solid symbols; stations with no samples containing Ra enrichment are shown by open symbols. Figure 9b is a temperature-salinity plot of the same samples. Note that the data for stations with Ra enrichments (solid symbols) plot along a mixing line of lower salinity than the data from stations without Ra enrichment (open symbols). The offset between these curves is in the range 0.2–0.6‰. This implies that the fluid producing the Ra enrichment is fresher than the ambient water. How much fresher could this fluid be without violating the salinity balance?

The product of the replacement time and Ra flux is well constrained by equation (1). Using a 20-day replacement time and a ^{226}Ra concentration of 5 dpm L^{-1} in the fluid yields a fluid flux of $4 \times 10^7 \text{ m}^3 \text{ d}^{-1}$. In this case the fluid will comprise 2% of the volume of the enriched zone. (The same result is obtained from a fluid flux of $8 \times 10^7 \text{ m}^3 \text{ d}^{-1}$ and a residence time of 10 days). If the salinity of the fluid is similar to the high-salinity well water, 17‰, it would dilute the ambient salinity in the enriched layer by 0.4‰. This is clearly in the 0.2–0.6‰ range of observed dilution (Figure 9b). We conclude that the Ra signal could have been produced by injection of a fluid similar in composition to the high-salinity groundwater we have measured; however, fluids quite different in composition could also produce the signal.

5.4. Source of Ra and Ba

It is likely that the encroachment and circulation of salt water in Tertiary aquifers are causing the Ra and Ba enrichments we observe offshore. The samples were collected in a karst terrain [Barans and Henry, 1984]. Nothing is known regarding encroachment into aquifers outcropping on the shelf, but encroachment of salt water into the Floridian aquifer farther south has been recognized for 50 years. To put the fluxes we calculate into perspective, we will consider the amount of Ra expected to be released through saltwater encroachment into the Floridian aquifer with the caveat that the Tertiary aquifer apparently outcropping in our study area may be responding to groundwater usage differently from the upper Floridian aquifer. Smith [1988] concluded that the seawater front was moving landward into the upper Floridian aquifer at a rate of 15–25 m yr^{-1} in the mid-1980s. The thickness of this intrusion is approximately 30 m. If this intrusion occurred along an 80 km segment of the aquifer, approximately 3×10^{11} grams of new sediment would be exposed to seawater each day. If this freshly exposed sediment released a third of its ^{226}Ra activity (~ 1 dpm g^{-1} [Elsinger and Moore, 1980]), the expected flux would be 1×10^{11} dpm d^{-1} . This estimate is of the same magnitude as the fluxes calculated from the enriched zone (2.4×10^{11} dpm d^{-1}). Of course, we are comparing two areas that may exhibit very different responses to changing groundwater flow patterns; and we do not yet have data on how the Ra flux varies throughout the year. More temporal data of Ra fluxes and estimates of saltwater encroachment specific to the study area are necessary to evaluate the Ra balance in the aquifer.

Table 2. Fluxes of ^{226}Ra , ^{228}Ra , and Ba Required to Support the Measured Enrichments in Bottom Waters for Different Bottom Water Replacement Times

| Replacement Time d | $Q_f C_f$ ^{226}Ra dpm d^{-1} | $Q_f C_f$ ^{228}Ra dpm d^{-1} | $Q_f C_f$ Ba mol d^{-1} |
|-----------------------|--|--|-------------------------------------|
| 10 | 4×10^{11} | 6×10^{11} | 2.4×10^9 |
| 20 | 2×10^{11} | 3×10^{11} | 1.2×10^9 |

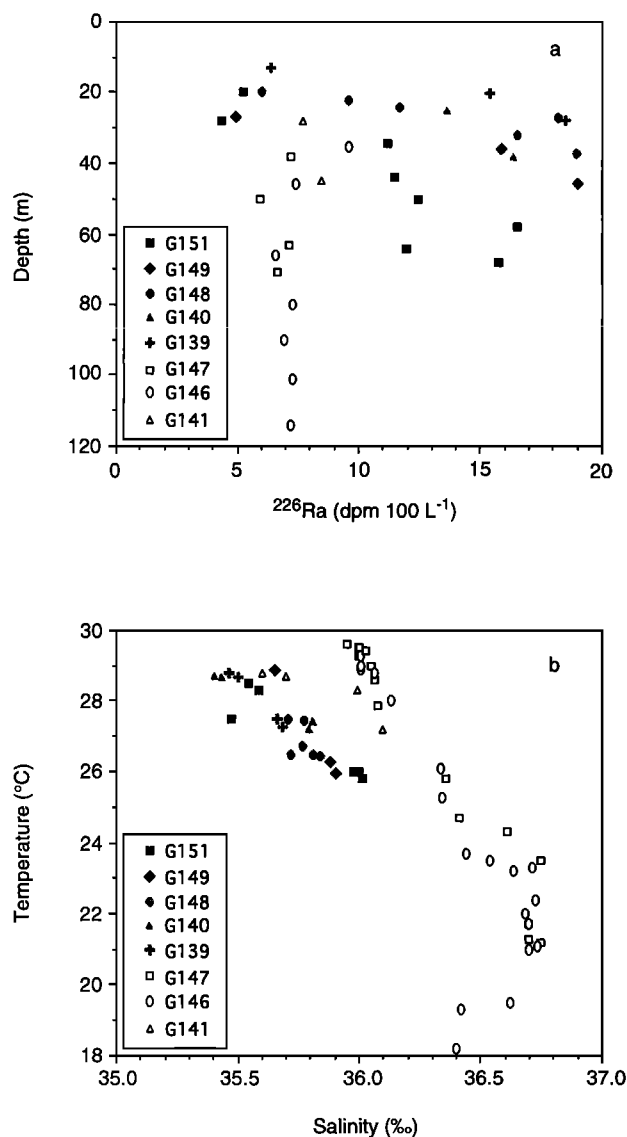


Figure 9. (a) A plot of ^{226}Ra versus depth shows that many samples in the 25-70 m depth range are enriched. Samples from stations having some samples enriched in Ra are shown by solid symbols. Samples from stations having no samples enriched in Ra are shown by open symbols. (b) A temperature versus salinity plot for the samples shown in Figure 9a reveals that stations with some samples enriched in Ra (solid symbols) follow a lower-salinity mixing line than stations having no enriched samples (open symbols).

5.5. Deep Fluorescence Signal

The pattern of elevated chlorophyll fluorescence in the bottom water on the shelf is similar to the enrichments of radium and barium in these waters. We interpret this to indicate that the advecting fluids supply nutrients to the bottom water and stimulate productivity. Water samples from the Floridian aquifer on land have ammonia concentrations of $30\text{--}180\ \mu\text{M kg}^{-1}$ and phosphate concentrations of $2\text{--}5\ \mu\text{M kg}^{-1}$ [A. Crotwell, personal communication, 1998]. If the fluids responsible for the Ra enrichment have similar nutrient concentrations, this could represent a considerable flux to the bottom waters. Because we did not measure nutrients in the bottom waters and because we do not know if the fluorescence signal represented ac-

tively growing phytoplankton cells, our interpretation remains speculative. The fluorescence signal could represent the remains of a surface water phytoplankton bloom that settled into the area or a bloom that originated farther offshore and grounded on the shelf. If either of these scenarios occurred, the signal we measured could have been a coincidence. We think our explanation is the most likely, but we cannot prove it.

6. Conclusion

1. Direct injections of subsurface fluids from coastal aquifers onto the outer continental shelf cause large chemical anomalies in the bottom water on the shelf.

2. These fluids are a mixture of groundwater and seawater that has reacted with aquifer solids. They are highly enriched in Ra and Ba relative to either endmember and depleted in salt relative to seawater. The injection of these fluids may cause local density inversions in the water column.

3. If the fluorescence signal represents chlorophyll related to *in situ* primary productivity, subsurface fluid injection has a significant impact on primary productivity on the middle and outer shelf.

4. Considering that only a small portion of the shelf has been surveyed for tracers of fluid flow, future studies will probably increase the flux estimate made here. Because other elements as well as Ra and Ba may be enriched by orders of magnitude in the fluids, the effect of fluid flow on the coastal ocean, indeed the whole ocean, may be enormous.

Acknowledgments. We thank Jim Krest, Mark Sochaski, Eron Higgins, Ioanna Stergiades, Robyn Kelly, and Amy Finelli for their assistance in the field and laboratory. Bob Key, two anonymous reviewers, and Kent Fanning provided comments that strengthened the paper. This research was supported by NSF grants OCE-9314587 and OCE-9712298.

References

- Atkinson, L. P., Hydrography and nutrients of the southeastern U.S. continental shelf, in *Oceanography of the Southeast U.S. Continental Shelf, Coastal Estuarine Sci.*, vol. 2, edited by L. P. Atkinson, D. W. Menzel, and K. A. Bush, pp. 77-92, AGU, Washington, D. C., 1985.
- Atkinson, L. P., and D. W. Menzel, Introduction: Oceanography of the southeast United States continental shelf, in *Oceanography of the Southeast U. S. Continental Shelf, Coastal Estuarine Sci.*, vol. 2, edited by L. P. Atkinson, D. W. Menzel, and K. A. Bush, pp. 1-9, AGU, Washington, D. C., 1985.
- Barans, C. A., and V. J. Henry, A description of the shelf edge groundfish habitat along the southeastern United States, *Northeast Gulf Sci.*, 7, 77-96, 1984.
- Cable, J. E., W. C. Burnett, J. P. Chanton, and G. L. Weatherly, Estimating groundwater discharge into the northeastern Gulf of Mexico using radon-222, *Earth Planet. Sci. Lett.*, 144, 591-604, 1996.
- Chan, L.-H., D. Drummond, J. M. Edmond, and B. Grant, On the barium data from the Atlantic GEOSECS expedition, *Deep Sea Res.*, 24, 613-649, 1977.
- Church, T. M., An underground route for the water cycle, *Nature*, 380, 579-580, 1996.
- Elsinger, R. J., and W. S. Moore, Ra-226 behavior in the Pee Dee River-Winyah Bay Estuary, *Earth Planet. Sci. Lett.*, 48, 239-249, 1980.
- Giffin, C., A. Kaufman, and W. S. Broecker, Delayed coincidence counter for the assay of actinon and thoron, *J. Geophys. Res.*, 68, 1749-1757, 1963.
- Hathaway, J. C., C. W. Poag, P. C. Valentine, R. E. Miller, D. M. Schultz, F. T. Manheim, F. A. Kohout, M. H. Bothner, and D. S. Sangrey, U.S. Geological Survey core drilling on the Atlantic shelf, *Science*, 206, 515-527, 1979.
- Johannes, R. E., The ecological significance of the submarine discharge of ground water, *Mar. Ecol. Prog. Ser.*, 3, 365-373, 1980.
- Key, R. M., J. L. Sarmiento, and W. S. Moore, Distribution of Ra-228 and Ra-226 in the Atlantic Ocean, technical report, Ocean Tracer Lab., Princeton, N. J., 1985.

- Klinkhammer, G. P., and L.-H. Chan, Determination of barium in marine waters by isotope dilution inductively coupled plasma mass spectrometry, *Anal. Chim. Acta*, 232, 323-329, 1990.
- Klinkhammer, G. P., and M. Palmer, Uranium in the oceans: Where it goes and why, *Geochim. Cosmochim. Acta*, 55, 1799-1806, 1991.
- Kohout, F. A., G. W. Leve, F. T. Smith, and F. T. Manheim, Red Snapper Sink and ground water flow off shore of southeastern Florida, in *Proceedings of the 12th International Congress, Karst Hydrogeology, Int. Assoc. Hydrogeol. Mem.*, 12, 193, 1977.
- Kohout, F. A., H. Meisler, F. W. Meyer, R. H. Johnston, G. W. Leve, and R. L. Wait, Hydrogeology of the Atlantic continental margin, in *The Geology of North America*, vol. I-2, *The Atlantic Continental Margin*, edited by R. E. Sheridan and J. A. Grow, pp. 463-480, The Geol. Soc. of Am., Boulder, Colo., 1988.
- Krest, J. M., and W. S. Moore, Ground-water radium in near-shore and salt marsh environments (abstract), *EOS Trans. AGU*, 77 (17), Spring Meet. Suppl., 153, 1996.
- Moore, W. S., Sampling ^{228}Ra in the deep ocean, *Deep Sea Res.*, 23, 647-651, 1976.
- Moore, W. S., Radium isotope measurements using germanium detectors, *Nucl. Inst. Methods*, 223, 407-411, 1984.
- Moore, W. S., Large groundwater inputs to coastal waters revealed by ^{226}Ra enrichments, *Nature*, 380, 612-614, 1996.
- Moore, W. S., and R. Arnold, Measurement of ^{223}Ra and ^{224}Ra in coastal waters using a delayed coincidence counter, *J. Geophys. Res.*, 101, 1321-1329, 1996.
- Moore, W. S., R. M. Key, and J. L. Sarmiento, Techniques for precise mapping of ^{226}Ra and ^{228}Ra in the ocean, *J. Geophys. Res.*, 90, 6983-6994, 1985.
- Moore, W. S., B. Kjerfve, and J. F. Todd, Identification of rain-freshened plumes in the coastal ocean using Ra isotopes and Si, *J. Geophys. Res.*, 103, 7709-7717, 1998.
- Oslund, G., H. Craig, W. S. Broecker, and D. Spencer, *GEOSECS Atlantic, Pacific, and Indian Ocean Expeditions: Shorebased Data and Graphics*, Nat. Sci. Found., Washington, D. C., 1987.
- Rama, and W. S. Moore, Using the radium quartet for evaluating groundwater input and water exchange in salt marshes, *Geochim. Cosmochim. Acta*, 60, 4645-4652, 1996.
- Shaw, T. J., W. S. Moore, J. Kloepper, and M. A. Sochaski, The flux of barium to the coastal waters of the southeastern United States: The importance of submarine groundwater discharge, *Geochim. Cosmochim. Acta*, in press, 1998.
- Simmons, G. M., Jr., Importance of submarine groundwater discharge (SGWD) and seawater cycling to material flux across sediment/water interfaces in marine environments, *Mar. Ecol. Prog. Ser.* 84, 173-184, 1992.
- Smith, B. S., Ground-water flow and saltwater encroachment in the upper Floridan aquifer Beaufort and Jasper Counties, South Carolina, *U.S. Geol. Surv. Water Resour. Invest. Rep. 87-4285*, 61 pp., 1988.
- Tsunogai, U., et al., Fresh water seepage and pore water recycling on the seafloor: Sagami Trough subduction zone, Japan, *Earth Planet. Sci. Lett.*, 138, 157-168, 1996.
- Valiela, I., J. Costa, K. Foreman, J. M. Teal, B. Howes, and D. Aubrey, Transport of groundwater-borne nutrients from watersheds and their effects on coastal waters, *Biogeochemistry*, 10, 177-197, 1990.
- Yoder, J. A., Environmental control of phytoplankton production on the southeastern U.S. continental shelf, in *Oceanography of the Southeast U.S. Continental Shelf, Coastal Estuarine Sci.*, vol. 2, edited by L. P. Atkinson, D. W. Menzel, and K. A. Bush, pp. 93-103, AGU, Washington, D. C., 1985.

W. S. Moore, Department of Geological Sciences, University of South Carolina, Columbia, SC 29208. (e-mail: moore@epoch.geol.sc.edu)

T. J. Shaw, Department of Chemistry and Biochemistry, University of South Carolina, Columbia, SC 29208. (e-mail: shaw@psc.sc.edu)

(Received June 30, 1997; revised June 15, 1998; accepted June 23, 1998.)